Image based reflectance measurement based on camera spectral sensitivities

Aditya Sole[1] , Ivar Farup[1] , and Shoji Tominaga[2] ;
1. The Norwegian Colour and Visual Computing Laboratory, Gjøvik University College, Gjøvik, Norway,
2. Graduate School of Advanced Integration Science, Chiba University, Chiba, Japan

Abstract

Image based measurement techniques are increasingly used to perform multi-directional reflectance measurements of objects/materials. In these techniques, commercially available colour (RGB) cameras are used along with the monochrome CCD cameras to measure the radiance reflected from the object/material surface at multiple reflection directions. The data acquired through these cameras is used to estimate the BRDF of given sample/material.

This paper presents an image-based method to measure the reflectance of the sample material using the camera spectral sensitivities. A multi-angle measurement setup described in previous studies was used to perform the measurements. A reflection model of the sample was derived in a colorimetric space using the Phong model. Camera spectral sensitivities were measured using a Bentham monochromator to build a tranformation from Camera RGB to CIEXYZ colour space. A reflection model was fitted in the colorimetric domain (CIEXYZ) for the sample materials used. Results show that image based multi-directional reflectance measurements can be performed using the camera spectral sensitivities.

Introduction

Multi-angle instruments and gonio-spectrometers are increasingly used to perform multi-directional measurements of radiance reflected from objects/materials (especially gonio-chromatic and non-diffuse object materials like metallic inks and special effect coatings). These instruments are precise and accurate and provide the measurements to calculate the bidirectional-reflection distribution function (BRDF) of a given objects/material. However, they are expensive, measure at fixed illumination and reflection angles and performing measurements is time consuming [1].

To overcome these drawbacks, image-based measurement techniques are increasingly used in performing multi-directional reflectance measurements of objects/materials [2, 3, 4]. These are fast and relatively cheaper. Monochrome CCD cameras or commercially available digital colour (RGB) cameras are used in these setups. The image captured using the colour camera records the light information in digital values [0 - 225] (for an 8-bit camera) for the individual camera sensors (R, G and B) also known as camera response C_k for that particular pixel.

The camera response C_k, for an image pixel, can be modelled using Equation (1).

$$C_k^j = \sum_i E(\lambda_i) \times R_j(\lambda_i) \times Q_k(\lambda_i)\Delta\lambda + n_k \qquad (1)$$

Where, C_k^j is the sensor response for the kth channel (R, G, B or monochrome) and for j^{th} pixel, n_k is the noise in the kth channel, Q_k is the spectral sensitivity function for the kth sensor channel, $E(\lambda)$ is the spectral power distribution of the illuminant, $R_j(\lambda)$ is the spectral reflectance imaged at pixel j, scalar $\Delta\lambda$ is the sampling step (in nm).

In order to compare measurements made using image based techniques to measurements performed using gonio-spectrometers or multi-angle spectrophotometers (which basically record the radiance reflected from the sample object in the spectral range 380nm - 730nm), we will have to either convert the camera captured R, G and B digital values to spectral or colorimetric values or convert the spectral reflectance values captured by the multi-angle spectrophotometers and gonio-spectrometers to camera RGB (digital) values.

For this conversion, it is important to know the camera spectral sensor sensitivity (Q_k) functions of the imaging device used in the measurement setup. Digital camera spectral sensitivity data being confidential is difficult to obtain from the camera manufacturer and is therefore needed to be either measured or estimated.

Looking at some of the work done till now in the area of digital camera spectral sensitivity measurements [5, 6, 7, 8, 9] we can observe that direct measurement of camera spectral sensitivity using a monochromator and a radiometer is much more accurate compared to estimation using colour patches with known spectral reflectance (for example using a ColourChecker test chart). However, the drawback in using the direct measurement approach is the time required, cost and availability of expensive equipment like monochromator and radiometers. Recently, a multi-primary image projector based camera sensitivity measurements system was introduced by Hirai et. al [10], where they used a multi-primary image projector to generate the monochromatic light which is used to measure the camera sensitivity. They used a one-shot-type camera spectral sensitivity measurement in which they reproduce rainbow projection for the measurement.

In this study we used a monochromator to measure the camera spectral sensitivities of the red (R), green (G) and blue (B) channels of the Nikon D200 camera. These measured camera sensitivities were further used in converting the camera RGB data to CIEXYZ colorimetric data. The camera spectral sensitivity measurement procedure and camera RGB to CIEXYZ conversion matrix estimation process is explained in the *Method's* section.

An image based multi-directional measurement setup as described in [4] was used to perform multi-angle colour measurements of a homogenous flexible packaging paper material. As discussed by us [4], modelling the reflection properties of mate-
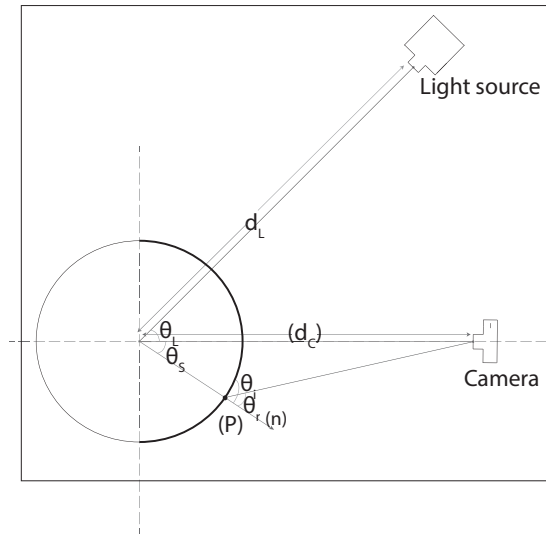
Figure 1. *Multi-angle measurement setup [4].*

Figure 2. *Schematic diagram of the camera sensor sensitivity measurement setup.*

Figure 3. *RAW image captured by camera at 610nm monochromatic light.*

rial surface is important for material appearance measurement and simulation and is used mostly in the computer graphics field to generate image simulations [11, 12, 13]. A reflection model was fitted using the Phong model to the data measured by the measurement setup. The Phong model is an empirical model with two surface reflectance components, one for diffuse surface (diffuse component) and one for specular surface (specular component) [11]. A three-dimensional light reflection using the Phong model can be described [14] as

$$H(\theta_i, \theta_r, \lambda) = S_a(\lambda)E(\lambda) + (\cos\theta_i)S_d(\lambda)E(\lambda) + \\ (\cos^\alpha(\theta_r - \theta_i))S_s E(\lambda) \tag{2}$$

$H(\theta_i, \theta_r, \lambda)$ is the radiance of light reflected from a surface and is a function of wavelenght (λ), including the illumination direction angle (θ_i) and the viewing angle (θ_r). $S_a(\lambda)$ is the ambient-spectral reflectance, $S_d(\lambda)$ is the diffuse-spectral reflectance of an object (diffuse component), S_s is the specular constant, and $E(\lambda)$ is the spectral power distribution of the light source. α is used as the measure of surface roughness.

Objectives

The objectives of the work presented in this paper are:

- to measure the sensor spectral sensitivity of the camera used as an imaging device in the multi-angle measurement setup. Obtaining these should help convert the camera RGB data to colorimetric/spectral space.
- to evaluate the measured sensor spectral sensitivity functions.
- to fit a reflection model in a colorimetric space using the camera measured data of the sample materials.
- to evaluate the reflection model.

Method
Sensor sensitivity measurement

As an imaging device in the multi-dimensional measurement setup, we used a commercially available Nikon D200 digital cam-
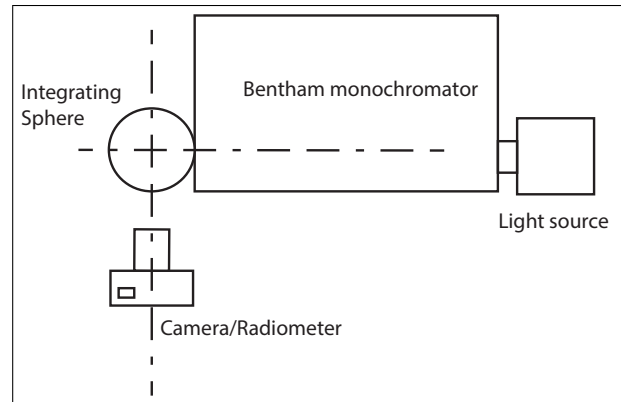
era to capture the light reflected from the samples. Spectral sensitivity of the 3 sensors (R, G and B) of the camera were measured.

In order to be precise and with limited access to a Bentham monochromator and Minolta CS1000 Tele-Spectro-Radiometer (TSR), we used the direct measurement approach to measure the spectral sensitivity of the Nikon D200. The 3 sensors' (R, G and B) sensitivity were measured by recording their responses to monochromatic light bands (narrow band wavelengths) using the monochromator. The measurements were performed in a dark-room. Figure 2 shows a schematic diagram of the measurement setup. The monochromator was mounted with a $BaSO_4$ coated sphere at the exit to have a uniform light output. The camera was positioned exactly in front of the sphere and focused. The distance between the camera and the sphere was adjusted in a way that the projected light was recorded in the center of the camera sensor array. Figure 3 shows an illustration of the RAW image captured by the camera of the monochromatic light projected at 610nm. RAW images of the monochromatic light ranging from 380nm to 730 nm at 10 nm intervals were captured by the camera.

Figure 4 shows the camera responses for the projected monochromatic light. After recording the projected light with the camera sensors, same was measured using the TSR to record the spectral power of the monochromatic light. For this, the
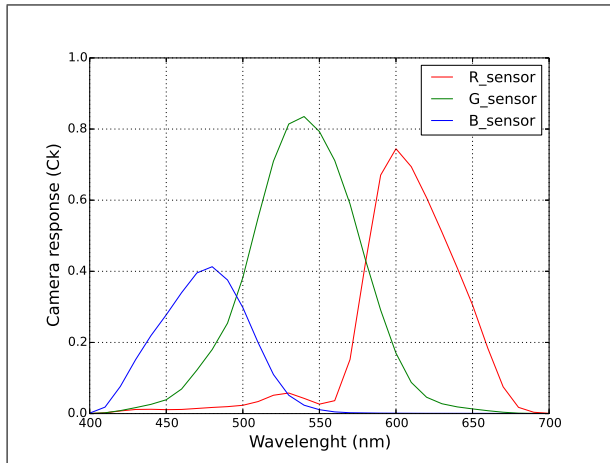
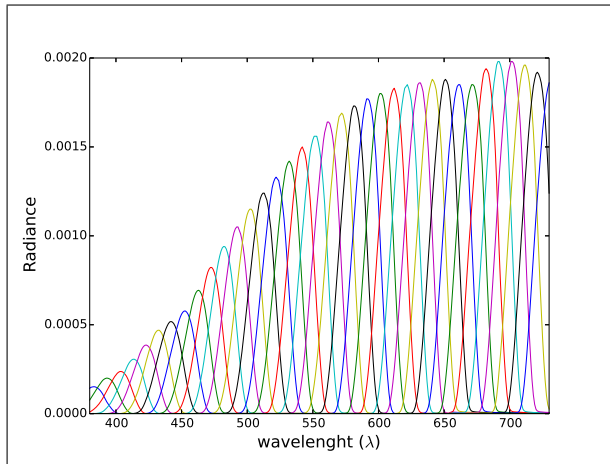**Figure 4.** *Camera response to monochromatic projections.*

Figure 5. *Spectral power distribution of monochromatic bands.*
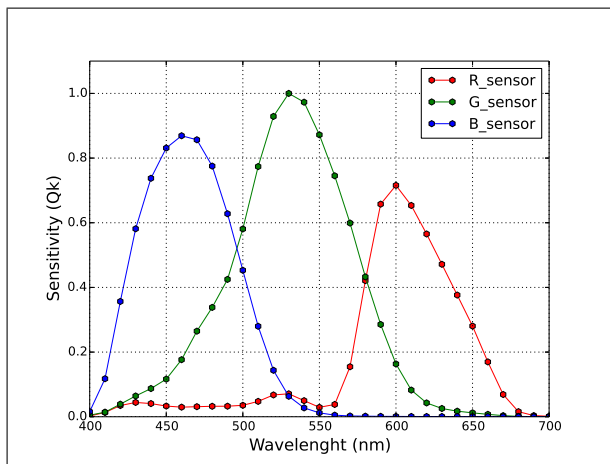

Figure 6. *Camera sensor sensitivity functions.*

camera was replaced with the TSR in the setup (refer Figure 2). Figure 5 shows the spectral power distributions measured by the TSR for all the monochromatic lights (400nm to 700nm at 10nm intervals) projected by the monochromator. In order to find out the actual band-width of the monochromatic bands projected by the monochromator, the Full Width at Half Maximum (FWHM) of the wavelength bandpass was calculated. Table 1 shows the maximum and minimum FWHM for the monochromatic bands used for the camera sensor measurements and the corresponding wavelength peak. The average bandwidth obtained was 22nm. This wide band-width was obtained due to slit limitations on the Bentham monochromator used in the sensor measurement process. According to ISO17321-1 [15], the bandpass of the monochromator to be used as an illuminating instrument shall be 5nm or narrower. However, due to limited access to the monochromator and the monochromator slitwidth limitations, the average minimum slit width obtained was approximately 22 nm. The camera response (see Figure 4) obtained for the

Table 1: Maximum and minimum FWHM of monochromatic bands that are used for camera sensor measurement

Monochromatic band peak (nm)	Bandwidth (nm)
410	20.3
670	23.3

monochromatic bands are dependent on the light source used by the monochromator. The camera sensor sensitivity is therefore calculated using the camera response and the spectral power distribution (SPD) measurements of the monochromatic bands made using the TSR. With reference to Equation (1), the camera response in this measurement procedure can be expressed as,

$$C_k(\lambda) = \sum_i Q_k(\lambda_i)L_k(\lambda_i)\Delta\lambda \tag{3}$$

where, C_k is the sensor response for the kth channel, $Q_k(\lambda)$ is the spectral sensitivity function for the kth sensor channel, $L_k(\lambda)$ is the spectral radiance. Assuming that the monochromatic band-pass $L_k(\lambda)$ has a narrow spectral power distribution compared to the sensor sensitivity in the same wavelength region, Equation (3) will be

$$C_k(\lambda) = Q_k(\lambda)\sum_i L_k(\lambda_i)\Delta\lambda$$
$$Q_k(\lambda) = \frac{C_k(\lambda)}{\sum_i L_k(\lambda_i)\Delta\lambda} \tag{4}$$

Figure 6 shows the camera sensor sensitivities calculated using Equation (4). The main aim of measuring the camera sensitivity functions was to be able to convert the camera RGB data captured using the multi-angle measurement setup to colorimetric space. To do so, we calculate a transformation matrix $\hat{M}$ using the camera sensor sensitivities ($r(\lambda)$, $g(\lambda)$, $b(\lambda)$) (estimated using Equation (4)) and the CIE 2° colour matching functions ($\bar{x}$, $\bar{y}$, $\bar{z}$) by minimising the error using the least square technique such as,

$$\hat{M} = \arg\min_M \|C - RM\|_F \tag{5}$$

where, C is a 31×3 matrix containing the CIE 2° colour matching functions, R is a 31×3 matrix of the camera sensitivities $(r(\lambda), g(\lambda), b(\lambda))$ estimated using Equation (4) (refer Figure 6). $\hat{M}$ will be a 3×3 matrix. Therefore the transformed colour matching functions ($\hat{C}$) will be,

$$\hat{C} = R\hat{M} \qquad (6)$$

In order to verify the accuracy of the transformation matrix $\hat{M}$ and the camera sensitivity measurements, we did capture a passport size 24 patches ColourChecker test chart. Figure 7 shows the captured image of the test chart using the Nikon D200 camera. The test chart patches were measured using the TSR (by replacing the camera with the TSR) in the same measurement conditions thus keeping the light source and, the illumination direction constant. Camera RGB data of the patches was transformed into CIEXYZ colour space using matrix $\hat{M}$. Similarly CIEXYZ values of the ColourChecker patches were computed from the radiance measurements made using the TSR and the transformed colour matching functions $\hat{C}$. CIEXYZ values were further converted to CIE $L^*a^*b^*$ colourspace using the Spectralon tile in the scene to compute the colour difference. Figure 8 shows a^* vs b^* plots of these 24 patches. An average $\Delta E_{a^*b^*}$ of 3.85 was obtained with the maximum at 8.21 for the cyan patch (refer Row1Column3 in Figure 7). Figure 9 shows a histogram plot of the colour difference in $\Delta E_{a^*b^*}$ for the ColourChecker patches.

Sample measurement

In this paper we used two materials as measurement samples that can be termed as homogeneous flexible packaging materials. The first sample was a 100% Cyan (C) colour patch and second was a 100 % Magenta (M) colour patch, both printed using wax based inks on matt coated white plotter paper using OCE Color-Wave 600 plotter.

These 2 samples were measured using the multi-angle measurement setup [4] at three illumination directions ($\theta_L = 24.5^\circ$, 31.5° and 37.6°). A tungsten point source was used as light source illuminating the sample and Nikon D200 DSLR camera as measurement sensor. Paper white (W) was also measured along with the samples (C) & (M).

Figure 10 shows the captured image of the sample at $\theta_L = 37.6^\circ$. Spectralon tile was used as reference white in the scene. The incident (θ_i) and reflection (θ_r) angles at given pixel points (P) were calculated for the 3 illumination directions (θ_L). Captured reflection data of the samples in terms of R, G and B intensities was then converted into CIEXYZ colour space using the transformation matrix $\hat{M}$. Figure 11 and 12 show the *CIEY* value for the corresponding reflection angles for the two samples (C) and (M) at $\theta_L = 24.5^\circ$ and $\theta_L = 37.6^\circ$.

Colorimetric Reflection Model

Measuring and modelling the reflection properties of an object material is important, if the material appearance of it needs to be reproduced using a 2.5D or 3D printing techniques or simulated using computer graphic techniques. Reflection models are used to estimate the reflection properties of these objects/materials. The surface-spectral reflectance of an object/material will vary with 1) the illumination, 2) viewing geometry and, 3) object's material composition [14].
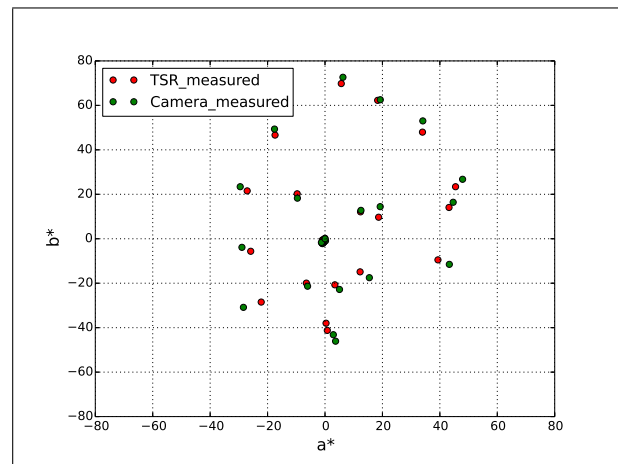

Figure 7. Captured ColourChecker test chart.

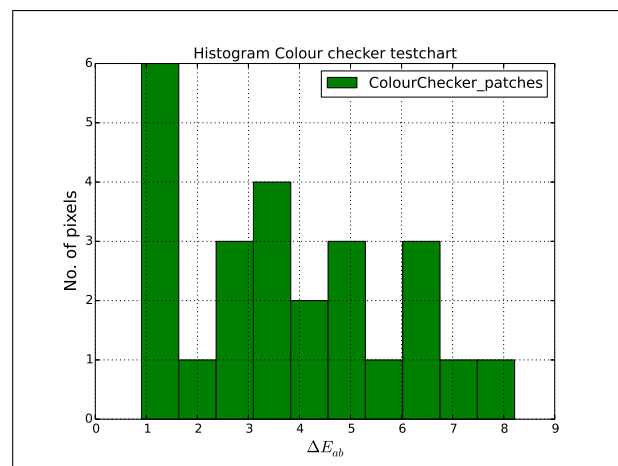**Figure 8.** $CIELAB_a^*$ Vs $CIELAB_b^*$ of the ColourChecker patches.

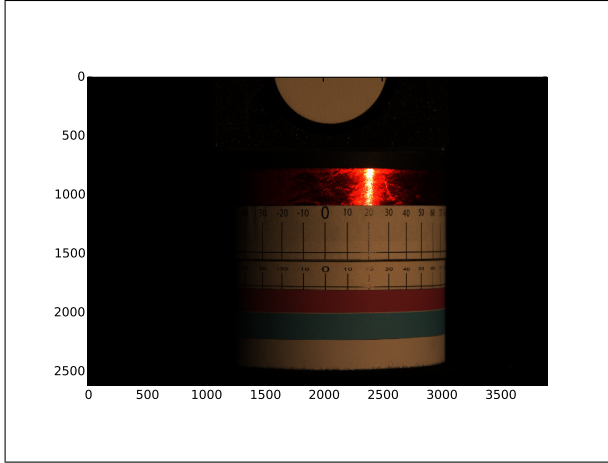**Figure 9.** $\Delta E_{a^*b^*}$ histogram of the ColourChecker testchart.
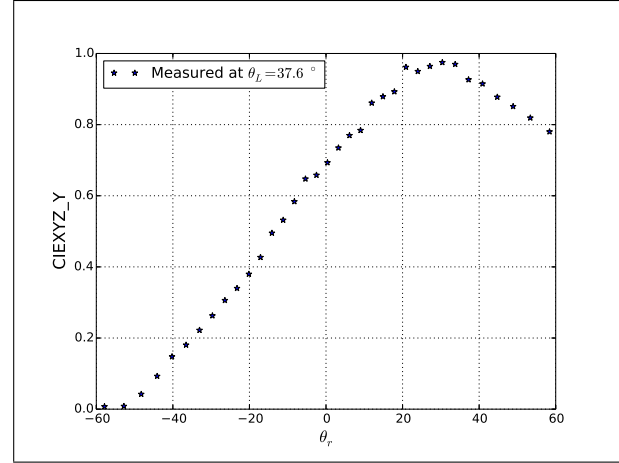
Figure 10. *Sample image captured at $\theta_L = 37.6°$.*

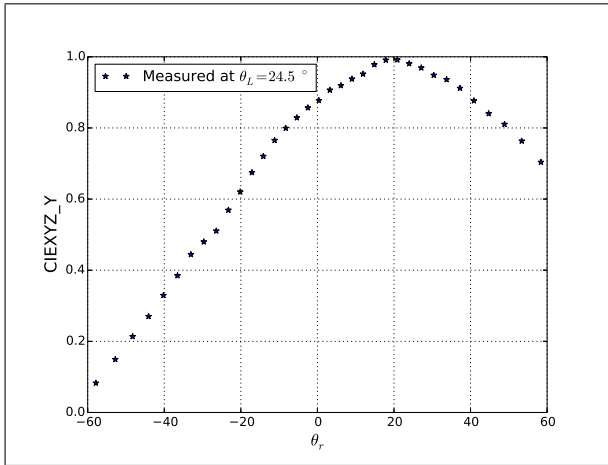**Figure 12.** *CIEXYZ Y value of (M) sample.*

Figure 11. *CIEXYZ Y value of (C) sample.*

The material (C) and (M) used being fairly diffuse we used the Phong model as described in Equation (2) to fit a reflection model for these two materials using the measured data. The Phong model has two components: *body reflectance* also known as diffuse component and *interface reflectance* known as specular component. This model describes the light reflection as a sum of interface and body reflection [14]. Colorimetric data (CIEXYZ) of the samples (C) and (M) (at multiple reflection angles) was obtained from the camera RGB using the conversion matrix $\hat{M}$. A reflection model was fitted in the CIEXYZ colour space using Equation (2) and the colorimetric data (CIEXYZ). As the data measured using RGB colour camera, was converted into the colorimetric space CIEXYZ using conversion matrix $\hat{M}$, referring to the measurement setup [4] and inserting the model parameters in Equation (2), the camera colorimetric output $H_{(X,Y,Z)}$ at spatial location p will be,

$$H_p = \begin{bmatrix} H_{p_X} \\ H_{p_Y} \\ H_{p_Z} \end{bmatrix} = k_a \mathbf{H_a} + k_d \mathbf{H_d}(\cos\theta_i) + k_s \mathbf{H_s}(\cos^\alpha(\theta_r - \theta_i)) \quad (7)$$

where, $\mathbf{H_a}$ is the ambient light vector, $\mathbf{H_d}$ is the diffuse component (body reflectance) vector proportional to $(S_d(\lambda)E(\lambda))$, $\mathbf{H_s}$ is

the specular component (interface reflectance) vector proportional to $E(\lambda)$, θ_i is the incident angle and θ_r the reflection angle. k_a, k_d, k_s are the ambient, diffuse and specular reflection coefficients and α is the coefficient for sample roughness.

As the measurements were performed in the darkroom conditions, the ambient light component $k_a \mathbf{H_a}$ was treated as zero. For the diffuse component, that is the body reflectance of the material, colorimetric values at normal to the camera sensor were used. Due to directional incident light, the measurements at normal to the camera sensor will have the maximum diffuse component and minimum specular component. The illumination light being directional ($\theta_L = 24.5°$, $31.5°$ and $37.6°$) the CIEXYZ values ($X_{d_{sample}}, Y_{d_{sample}}, Z_{d_{sample}}$) at the center pixel of the camera sensor were used as the body reflectance component $\mathbf{H_d}$. In theory the specular component of the light source will be maximum reflected from the surface of an object/material at $\theta_i = \theta_r$. Therefore, for the specular component $\mathbf{H_s}$ in the reflection model, we used the CIEXYZ values ($X_{s_{white}}, Y_{s_{white}}, Z_{s_{white}}$) corresponding to pixel position (p) at $\theta_i = \theta_r$ for the given illumination direction (θ_L). Inserting the diffuse and specular component values in Equation (7),

$$H_p = \begin{bmatrix} H_{p_X} \\ H_{p_Y} \\ H_{p_Z} \end{bmatrix} = k_d \begin{bmatrix} X_{d_{sample}} \\ Y_{d_{sample}} \\ Z_{d_{sample}} \end{bmatrix} \cos\theta_i + k_s \begin{bmatrix} X_{s_{white}} \\ Y_{s_{white}} \\ Z_{s_{white}} \end{bmatrix} \cos^\alpha(\theta_r - \theta_i)$$

$$(8)$$

Reflection coefficients k_d, k_s and roughness coefficient α were fitted and optimized in Equation (8) using the colorimetric data (CIEXYZ) calculated from the camera measurements performed at the 3 illumination directions (θ_L). Nelder-Mead downhill simplex algorithm [16] was used to optimize the coefficients using the function,

$$Total_{Err_{XYZ}} = \sum_{\theta_L=0}^{M} \sum_{P=0}^{N} \Delta XYZ \quad (9)$$

where,
$\Delta XYZ = \sqrt{(X_{mea} - X_{est})^2 + (Y_{mea} - Y_{est})^2 + (Z_{mea} - Z_{est})^2}$, $X_{mea}, Y_{mea}, Z_{mea}$ are the CIEXYZ values used to fit the reflection

model using Equation (8),

$X_{est}, Y_{est}, Z_{est}$ are the CIEXYZ values estimated by the reflection model,

p is the total number of pixel values (N) and,

θ_L is the illumination directions ($\theta_L = 24.5°$, $31.5°$ and $37.6°$, that is M = 3). As the measurement data used to fit the reflection model is in the colorimetric colour-space, CIE X, Y and Z data corresponds to the same pixel in the image. We, therefore, use the Euclidean error (ΔXYZ) to minimize the total error. Table 2 shows the coefficients k_d, k_s and α fitted for the two samples (C and M) using Equation (8) and (9).

Table 2: Phong reflection model fitting parameters and LRMS error

Material	K_d	K_s	α	RMSE
C	0.6831	0.0527	1.033	0.10
M	1.4601	0.0766	1.9132	0.11

Results

Table 3: Colorimetric difference in $\Delta E_{a^*b^*}$ between camera measured and the Phong model estimated data

Material	θ_L	Average $\Delta E_{a^*b^*}$	Maximum $\Delta E_{a^*b^*}$
	24.5°	1.15	1.59
C	31.5°	1.36	2.15
	37.6°	1.39	2.36
	24.5°	1.36	2.17
M	31.5°	1.65	2.36
	37.6°	1.60	2.65

Figures 13, 14, show the plots for the camera measured and reflection model estimated CIE Y value for 2 incident light directions (θ_L=24.5°, 37.6°). From the plots it can be observed that the reflection model fitted to the data in the colorimetric space works well. In order to evaluate the accuracy of the model in colorimetric space, the CIEXYZ values measured by the camera and estimated by the reflection model were transformed into CIE $L^*a^*b^*$ values using the spectralon tile measurements made using a tele-spectro-radiometer. Colorimetric wise we get a good fit using the model with an average $\Delta E_{a^*b^*}$ of 1.3 for cyan (C) sample whereas 1.54 for magenta (M) sample in the reflection angle range of $\theta_r = -60°$ to $+60°$ where the camera sensor is normal to the sample at $\theta_r = 0°$. Table 3 shows the average and maximum colorimetric differences for the sample materials in the same reflection angle range at the three illumination directions (θ_L). Figure 15 and 16 show the histogram plot for of the $\Delta E_{a^*b^*}$ for both the samples.

Conclusion and Discussion

We presented an image-based method to measure the reflectance of the sample material using the camera spectral sensitivity. Bentham monochromator was used to measure the camera spectral sensitivities. The FWHM for the monochromatic band-pass used was approximately 22nm. Due to limited access to the measurement setup a smaller exit slit on the monochromator could not be used.
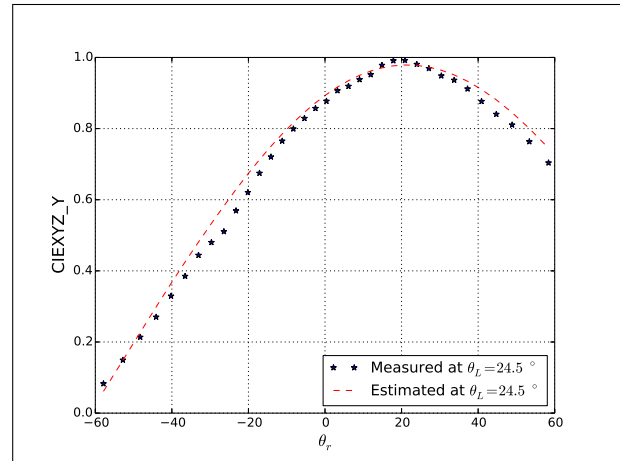

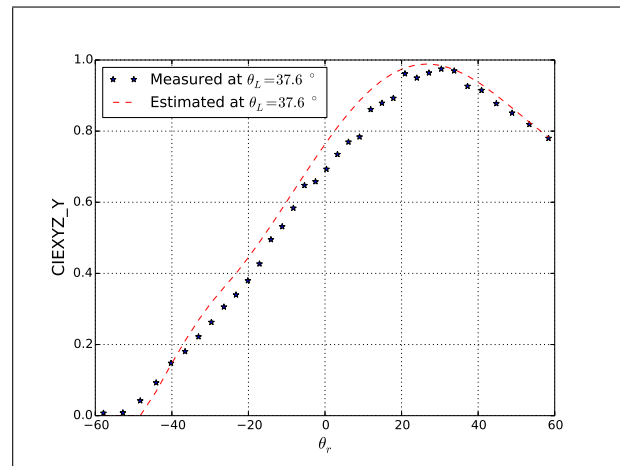**Figure 13.** CIEXYZ Y value of (C) sample measured and estimated at $\theta_L = 24.5°$.

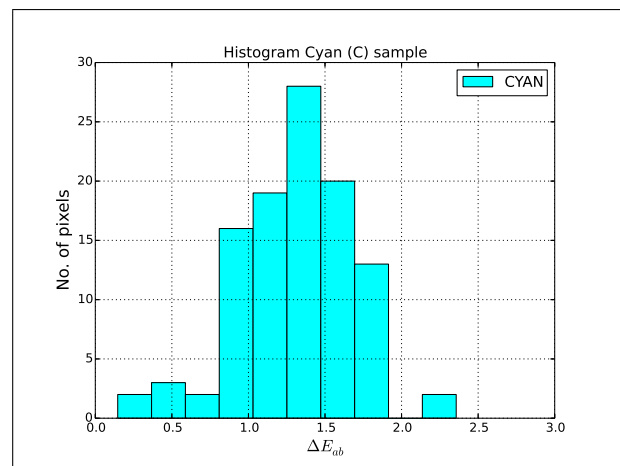**Figure 14.** CIEXYZ Y value of (M) sample measured and estimated at $\theta_L = 37.6°$.

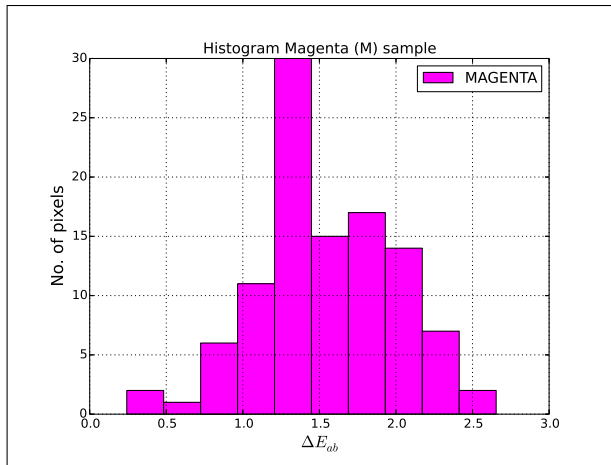**Figure 15.** $\Delta E_{a^*b^*}$ histogram of Cyan (C) sample.

Figure 16. ΔE_{a*b*} histogram of Magenta (M) sample.

An important point to note in this study is that we estimated the camera spectral sensitivity with the assumption that the monochromatic bandpass used is narrow enough compared to the sensor sensitivity in the same wavelength region. However, looking at the sensitivity measurements (refer Figure 6) we can observe that this assumption does not hold true for all wavelengths considered in the measurement (i.e. 400 - 700 nm). This will possibly add to the error in the camera sensitivity measurements. If the monochromatic bandpass was narrower (say 5 nm) we should have obtained more sharper sensitivity curves compared to what we have obtained now. A transformation matrix $\hat{M}$ was estimated using the camera sensitivity measurements R and CIE $2°$ colour matching functions. The sensitivity measurements and transformation was evaluated using a ColourChecker test chart. Looking at the colorimetric difference we can conclude that the performance of the transformation is acceptable and can be used in the reflectance measurement setup.

As the measurement samples used were fairly diffuse, the colorimetric reflectance model was derived using the Phong model. Using the transformation matrix $\hat{M}$, the camera captured data was converted into the colorimetric space (CIEXYZ) and the reflection model was fitted in the CIEXYZ colourspace. The advantage of fitting the reflection model in the colorimetric space is that, the directional reflectance properties of the samples used can be simulated/estimated directly into the colorimetric space. This should support in visualisation of the colour data in the perceptual domain to help understand how we perceive directional colour.

From the results obtained we can conclude that the reflection model works satisfactorily and the sample colorimetric values can be estimated at multiple directions using the proposed model for the sample materials used in this study.

A point to note is that in this study, same measurement dataset is used to train and test the reflection models for both the samples. This can also be considered as one of the reasons to get a good fit between the estimated and measured data. As part of future work the model will be verified using a measurement dataset different than the training dataset. The measurement setup and reflection model will also be verified against measurements performed using a gonio-spectrometer. This should possibly help us validate the measurement setup against reference gonio-measurement instruments like spectro-spectrometers and multi-angle spectrophotometers.

Acknowledgments

References

[1] G. Baba, "Gonio-spectrophotometry of metal-flake and pearl-mica pigmented paint surfaces," in *Proceedings of the fourth Oxford conference on spectrophotometry*, pp. 79–86, SPIE, 2003.

[2] J. Rong Lu, J. Koenderink, and A. M. L. Kappers, "Optical properties (bidirectional reflection distribution functions) of velvet," *Applied Optics*, vol. 37, pp. 5974 – 5984, September 1998.

[3] S. R. Marschner, S. H. Westin, E. P. F. Lafortune, K. E. Torrance, and D. P. Greenberg, "Image-based brdf measurement including human skin," in *10th Eurographics Workshop on Rendering*, pp. 139 – 152, 1999.

[4] A. S. Sole, I. Farup, and S. Tominaga, "An image-based multi-directional reflectance measurement setup for flexible objects," in *Measuring, Modeling and Reproducing Material Appearance 2015* (M. V. O. Segovia, P. Urban, and F. H. Imai, eds.), vol. SPIE 9398, pp. 93980J – 93980J–11, Proceedings of SPIE-IS& T Electronic Imaging, 2015.

[5] M. M. Darrodi, G. Finlayson, T. Goodman, and M. Mackiewicz, "Reference data set for camera spectral sensitivity estimation," *J. Opt. Soc. Am. A*, vol. 32, pp. 381–391, Mar 2015.

[6] J. E. Farrell, P. B. Catrysse, and B. A. Wandell, "Digital camera simulation," *Appl. Opt.*, vol. 51, pp. A80–A90, Feb 2012.

[7] J. Y. Hardeberg, *Acquisition and reproduction of colour images: colorimetric and multispectral approaches*. PhD thesis, Ecole Nationale Superieure des Telecommunications, 1999.

[8] M. M. Darrodi, G. Finlayson, T. Goodman, and M. Mackiewicz, "A ground truth data set for nikon camera's spectral sensitivity estimation," *Color and Imaging Conference*, vol. 2014, pp. 85 – 90, November 2014.

[9] J. Farrell, M. Okincha, and M. Parmar, "Sensor calibration and simulation," in *Digital Photography IV* (J. M. DiCarlo and B. G. Rodricks, eds.), vol. 6817, pp. 68170R–68170R–9, Proceedings of SPIE-IS& T Electronic Imaging, 2008.

[10] K. Hirai, D. Irie, and T. Horiuchi, "Photometric and geometric measurements based on multi-primary image projector," in *Colour and Visual Computing Symposium (CVCS), 2015*, pp. 1 – 5, August 2015.

[11] B. T. Phong, "Illumination for computer generated pictures," *Commun. ACM*, vol. 18, pp. 311–317, June 1975.

[12] J. F. Blinn, "Models of light reflection for computer synthesized pictures," in *Proceedings of the 4th Annual Conference on Computer Graphics and Interactive Techniques*, SIGGRAPH '77, (New York, NY, USA), pp. 192–198, ACM, 1977.

[13] R. L. Cook and K. E. Torrance, "A reflectance model for computer graphics," *ACM Trans. Graph.*, vol. 1, pp. 7–24, Jan. 1982.

[14] S. Tominaga, "Dichromatic reflection models for rendering object surfaces," *Journal of Imaging Science and Technology*, vol. 40,

x